International Journal of Current Engineering and Technology
E-ISSN 2277 – 4106, P-ISSN 2347 – 5161

Available at http://inpressco.com/category/ijcet

Research Article

Dynamic and thermal analysis of a hybrid solar collector

ABIDI Sihem[1*], SAMMOUDA Habib[2] and BENNACER Rachid[3]

[1,2]LabEM, LR11ES34-Université de Sousse, Ecole Supérieure des Sciences et de Technologie, Rue Amin ElAbbassi, 4011 Hammam Sousse (Tunisie)
[1]University of Hafer Al Baten- Physics Department
[3]ENS-Cachan, LMT, Dpt GC 61, Av. Président Wilson 94235 Cachan Cedex, France

Received 15 Nov 2022, Accepted 02 Dec 2022, Available online 05 Dec 2022, **Vol.12, No.6 (Nov/Dec 2022)**

Abstract

In order to improve the performance of the hybrid photovoltaic/thermal system; we proposed to associate a sensor of solar photovoltaic cells to an exchange. The exchanger is constituted by the two fluids which are separated by the solid wall. The aims of this work are to recuperate the maximum of energy lost by Joule effect using the coolant in contact with photovoltaic cells (fluid 1). The convection and the conduction modes of transfer are established in the level of the roof of the local cavity which filled with air (fluid 2). The phenomena of the heat and the mass transfer have been studied and simulated to obtain the thermal and dynamical fields. The effects of the nature of fluids and of the thermal conductivity of solid are analyzed on the behaviors of coolants and on the efficiency of censor. Results suggested that a better operating performance can be obtained for such system if we optimized the nature and the dimension of coolants (fluid 1) and that of solid wall. The use in the present work, of air as fluid 1 and of a variety of fluid 2, (gallium, EVA, air), proved the necessity of optimize the values of the parameters characterizing this system. In effect, that could efficiently generate electricity and thermal energy simultaneously while keeping a moderate temperature to PV cells.

Keywords: *Component Convection; Heat Exchanger; sensor Solar PV cells; coolant*

Introduction

Solar energy is distinguished from other resource-based carbon, low pollution and sustainable availability. Every day the sun sends to the earth more energy than the 6 billion inhabitants of the planet consume in 25 years. This resource is inexhaustible on a human scale; however, it is still largely untapped. But the PV cells presented some drawbacks such as the heating of the cell temperature junction and the low PV sensors yield (20 %).

Basak. K.k et al. [1] Presented a comparison of Trombe wall system between a single glass PV panel and another with a double glass. After validation of the numerical models with the experimental results, these systems will be used in a building in different climatic conditions, glass types and thermal masses. Furthermore, they noted that the temperature reached by PV cells is higher than the ambient temperature and that the efficiency of PVTs is greater than the combined sum of separate PV and thermal collectors. In the light of this, they suggest that PVT systems offer a cost effective solution for applications where roof area is limited.

D. Kamthania et al. [2] evaluated the performance of a hybrid PVT double pass facade for space heating in the composite climate of New Delhi by using a semi transparent PV module. Thermal modelling has been carried out based on the first and second law of thermodynamics in order to estimate the electrical and thermal energy along with the exergy for a "semi-transparent" hybrid PVT double pass façade instead of an opaque PV panel. In the light of this, they suggested that the semi transparent PV module has more electrical efficiency than the opaque PV module. F. Sarhaddi et al. [3] evaluated the exergetic performance of a solar PV/T air collector and carried out the detailed energy and exergy analysis to calculate the thermal and electrical parameters, exergy components and exergy efficiency of a typical PV/T air collector. I.R. Caluianu et al. [4] developed and validated, using experimental data, a BP 585 F photovoltaic panel thermal model. They made a simulation by applying the galerkin finite element method to the flow and energy equations, incorporating an implicit convective boundary condition. The values of the root mean square error and the correlation coefficient between the experimental and the simulated values of the panel temperature show a good accuracy of the model.

*Corresponding author's ORCID ID: 0000-0000-0000-0000
DOI: https://doi.org/10.14741/ijcet/v.12.6.3

Afterwards, this was used to simulate the convective flow between the photovoltaic module and the roof wall. The influence of this channel width was then studied. Velocity and temperature variations were calculated at the beginning, the middle and the exit of the channel for 10 mm, 20 mm and 30 mm width. A. Ibrahim et al. [5] made the comparison of the device each type of the flat plate PV/T collectors and performance of each type. Besides that, this paper provides reviews of the latest development and the future work on the PV/T collector based on previous researcher's review. This work also convoluted the principal classifications of flat plate PVT collectors systems. This classification provides clearly how this flat plat PV/T collector system designed can be grouped systematically according to the type of working fluid used such as water or air. An interesting attempt has been made by Anderson et al. [6] to integrate the PV/T system to a building. In this experiment, PV cells are laid onto a standing seam or troughed sheet roof using a laminated technique to a BIPVT system. The designed BIPVT system allowed the water to pass through underneath the cells to generate hot water when exposed to the heat from the sun. The result from this experiment showed that the design parameters included the fin, the conductivity between the cells, the roofing material and also the laminating technique influenced the BIPVT system. They strongly believed that the BIPVT could be made cheaper even when using a common pre-coated colour steel material. GL. Jin et al. [7] developed an experiment on a single-pass PV/T with a rectangular tunnel absorber. The rectangular tunnel which acted as an absorber collector has been fixed underneath the photovoltaic panel. The main purpose of the experiment is to identify a suitable air flow for cooling the PV panel. By doing this, the efficiency of the panel will increase. The result showed that the combined PV/T efficiency was 64.72% and the thermal efficiency at 54.70% with solar irradiance of 817.4Wm-2, and the mass flow rate reached 0.0287kgs-1 at ambient temperature of 25°C. They concluded that the hybrid PV/T with a rectangular tunnel as a heat absorber showed a higher performance compared to the conventional PV/T system. Bolcken et al. [8] and Defraeye et al. [9] verified the importance of near-wall modelling for CHTC prediction at building surface and reported overestimations with standard and non-equilibrium wall functions (WF) that can be up to 60% and 30%, respectively. For the windward façade of a cubic building, they did not resolve the viscous sub-layer and the buffer layer (where the largest resistance to surface heat and mass transfer is embedded). Karava et al. [10] developed accurate thermal analysis models for the design and control of building-integrated Photovoltaic/Thermal (PV/T) systems. Since the convective heat transfer between the roof and the external airflow has a significant impact on the electrical and thermal efficiency of the system. The main objective of this paper is to evaluate the CHTC for the inclined roof surfaces of low-rise buildings. Specifically, the aim is to develop, for the first time, dimensionless correlations for the CHTC that take into account the effects of the building/roof geometry and the incident atmospheric boundary layers on the roof velocity and thermal boundary layers, notably the terrain roughness length and the turbulence intensity at eaves height. R.Daghigh et al. [11] presented the more detailed studies of a new design of an absorber collector under the meteorological conditions of Malaysia (hot and humid climate). Since few studies of BIPVT water based systems especially amorphous silicon systems have been conducted up to now, therefore further experimental and numerical work should be carried out aiming at incrementing our knowledge regarding improving electrical performance and thermal efficiency of PV/T solar collector using a new design of absorber collector. In the work of A. Ibrahim et al. [12], seven configurations of new sensors absorption PV/T were designed, investigated and compared. Simulations were performed to determine the best absorber design that gives the highest efficiency (total efficiency). In these simulations, the system was analysed with various parameters, such as solar radiation, ambient temperature, and flow rate conditions. It was assumed that the collector was represented as a flat thermal collector with a single glazing sheet. Based on these simulations, spiral flow design proved to be the best design with the highest thermal efficiency of 50.12% and a corresponding cell efficiency of 11.98%. Roman and Tiwari [13, 14] studied the annual thermal and exergy efficiency of the PVT/a collector for five different Indian climate conditions. It was observed that the exergy efficiency is 40-45% lower than the thermal efficiency under strong solar radiation. Also the double-pass design shows a better performance than the single-pass option. S. Dubey et al. [15] studied different configurations of glass-to-glass and glass-to-tedlar PV modules. Analytical expressions for electrical efficiency with and without airflow were developed as a function of climatic and collector design parameters. Experiments at the Indian institute of technology, Delhi found that the glass-to-glass type is able to achieve a higher supply of air temperature and electrical efficiency. This is because the radiation that falls on the non-packing area of the glass-to-glass module is transmitted through the front cover. It's average PV efficiencies with and without duct were determined 10.4% and 9.75%, respectively. Hence a difference of about 0.7%. The percentage differences between the PV efficiency of the glass-to-glass and that of the glass-to-tedlar type were respectively, 0.24% with duct and 0.086% without duct. In Hong Kong, Chow et al. [16] carried out outdoor measurements on two identical sheet-and-tube thermosyphon PVT/w collector systems, in which one was glazed. Together with a validated numerical model, the appropriateness of having front glazing was evaluated. The first law of thermodynamic evaluation indicates that the glazed design is always suitable

whether the thermal or the overall energy output is to be maximised, but the exergy analysis supports the use of unglazed design if the increase of PV cell efficiency, packing factor, ratio of water mass to collector area and wind velocity are seen as desirable factors.

The objective of our work is to study the effect of an additional pane on the thermal performance, the influence of air flows. Then we will study the effect of the thermal conductivity of the metallic absorber on the most optimal system performance. Thus, we study the efficiency of the overall system using steady values of characteristic numbers, Ra, heat flux captured, Re, air flows, and λ, the thermal conductivity of the solid absorber. This system is made up of a cavity enclosing a first coolant fluid with an open channel and a second driving coolant (air), the wall adjacent to the cavity is an absorber solid of high thermal conductivity. Above this system we add an additional pane, as shown schematically in Fig. 1.

Mixed convection heat exchanger

In order to optimize the efficiency of the photovoltaic sensor and that of the heat exchanger, it is proposed to use the heat lost by Joule effect to heat the air injected into a vertical channel.

The configuration considered is that of a PVT hybrid solar photovoltaic sensor (PV sensor + exchanger) used to heat a fluid passing through a channel where a mixed convection flow regime prevails (FIG. 1). Thus the flow rates of the heat transfer fluid within the PV sensor and the exchanger will be influenced by these characteristic parameters ***Ra₀*** (solar flux captured by the PV panel), ***Re*** (rate of injection of air into the channel), as well as ***λ*** (the thermal conductivity of the metal wall).

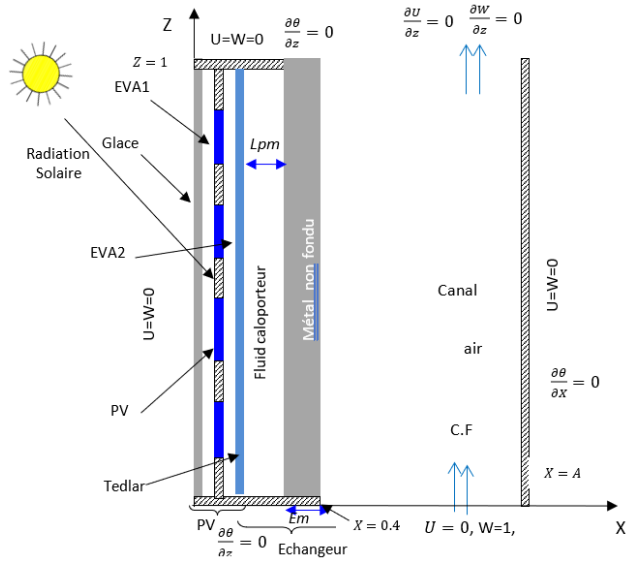

Figure 1: PV sensor associated to heat exchanger Configurations

Governing Equations

The movement of the fluids and their temperature are governed by continuity, momentum and energy equations in the solid and fluid phases. The heat flux imposed on the up boundary is considered only on the level of PV cells, with density G". Thus, the reference variables for length, velocity and temperature are chosen respectively as:

$$X=\frac{x}{H};Z=\frac{z}{H}\ ;\ \text{and}\ V_{ref}=\frac{\vartheta}{H}$$

The dimensionless variables are: $\theta=\frac{T-T_a}{\Delta T}$ and $\overrightarrow{V}(U,W)$

The dimensionless conservation equations of mass and momentum for the dimensionless natural convection flow of fluid are:

❖ On the level of the fluid:

$$\overrightarrow{\nabla}.\vec{V}=0$$

❖ Natural convection

$$(\vec{V}.\vec{\nabla})\vec{V}=-\vec{\nabla}P+Gr_{Ti}\theta_{fi}\overrightarrow{e_g}+\Delta\overrightarrow{V}$$
$$\overrightarrow{e_g}=-cos\gamma\vec{\imath}-sin\gamma\vec{\jmath}$$
$$\overrightarrow{V}.\vec{\nabla}\theta_{fi}=\frac{1}{Pr_i}\vec{\nabla}.\vec{\nabla}\theta_{fi}$$

✓ Mixed convection

$$(\vec{V}.\vec{\nabla}).\vec{V}=-\vec{\nabla}P+\frac{Gr_{Ti}}{Re^2}\theta_{fi}\overrightarrow{e_g}+\frac{1}{Re}\Delta\overrightarrow{V}$$
$$\overrightarrow{V}.\vec{\nabla}\theta_{fi}=\frac{1}{Pr_iRe}\vec{\nabla}.\vec{\nabla}\theta_{fi}$$

❖ On the level of the solid exchanger:

$$\overrightarrow{\nabla}.(\vec{\nabla}\theta_s)=0$$

❖ At the interface solid/fluid

$$\overrightarrow{\nabla}.(\vec{\nabla}\theta_s)=Bi(\theta_s-\theta_f)$$

Boundary conditions

If we note by $\vec{V}(U,W)$ the velocity vector and by θ the temperature, the dimensionless boundary conditions are written;

A (X = 0, 0 ≤ Z ≤ 1): U = 0, W = 0 et $\frac{\partial\theta}{\partial X}=1$, Solar flux

A (X = A, 0 ≤ Z ≤ 1): U = 0, W = 0 et $\frac{\partial\theta}{\partial X}=0$, adiabatic condition

A (Z = 0) { U = 0, W = 0 et $\frac{\partial\theta}{\partial Z}=0$, (0 ≤ X ≤ 0.4), (adiabatic condition)

$U = 0$, $W = 1$ et $\theta = 0$, $(0.4 \leq X \leq A)$, (input channel)

A (Z = 1) { U=0, W=0 et $\frac{\partial \theta}{\partial Z} = 0$, $(0 \leq X \leq 0.4)$, (adiabatic condition)
$\frac{\partial U}{\partial Z} = 0$ et $\frac{\partial W}{\partial Z} = 0$, $(0.4 \leq X \leq A)$, (output channel)

- Fluid / solid interface, at X=X0 and $0 \leq Z \leq 1$:

$$\vec{\nabla}\theta_f/_{X=X_0} = \frac{Bi}{R_\lambda}\left(\theta_f(X_0, Z) - \theta_s(X_0, Z)\right)$$

$$Bi = \frac{hH}{\lambda_s}; \quad R_\lambda = \frac{\lambda_f}{\lambda_s}$$

- Fluid / solid interface, at X=X1 et $0 \leq Z \leq 1$:

$$\left(\vec{\nabla}\theta_s\right)/_{X=X_1} = Bi\left(\theta_s(X_1, Z) - \theta_f(X_1)\right)$$

We used, for this configuration, an irregular mesh of (121,121) nodes judged having no effect on the results. Convergence is reached when the residue is less than a predetermined value, generally taken equal to 10-6.

Results and discussions

The governing Eqs. 1-4 with the boundary conditions were solved using the finite volume method. The computational domain is divided into rectangular control volumes with one grid point located at the centre of the control volume that forms a basic cell. The conservation equations are integrated in the control volumes, leading to a balance equation for the fluxes at the interfaces. A second order scheme is used to distinguish the equations; a false transient procedure is used in order to obtain a permanent solution. To accelerate the convergence, the SIMPLER algorithm, originally developed by Patankar [17], is coupled with the SIMPLEC algorithm of van Doormaal and Raithby [18] (see Bennacer [19]). Non uniform grids are used in the program, allowing fine grid spacing near the boundaries. Trial calculations were necessary to optimize the computation time and accuracy. Convergence with mesh size was verified by using coarser and finer grids for selected test problems. The convergence criterion is based on both the maximum error of continuity equation and the average quadratic residue over the whole domain for each equation being less than a prescribed value ζ (generally less than 10-6).

The aim of the present study is to be interested in recovering waste heat by Joule effect by adding the sensor PV exchanger three coolants and demonstrating the optimum of performance of the system in both electrical (junction temperature of the PV) and thermal (temperature of the hot air recovered at the outlet of the channel). The heat quantity transferred, at position z, is calculated from the average Nusselt number, Nu (z), a long x direction, defined as: $Nu(z) = \frac{1}{A}\int_0^A Nu(x,z)dx$

And the average Nusselt number, $Nu = \int_0^1 Nu(z)dz$

Where $Nu(x,z) = -\left(\frac{\partial\theta(x,z}{\partial x}\right) + W(x,z)\theta(x,z)$ the local heat transfer at any point. Where W is the velocity component along Z axis.

Validation of numerical model

In order to obtain a grid independent solution, a grid refinement study is performed for three zones. Fig. 2 shows the effect of the grid refinement on the global heat transfer flux (average Nusselt number, Nu). It is noted that the results are unchanged beyond (41*121) grid, we choose the (51,121) grid.

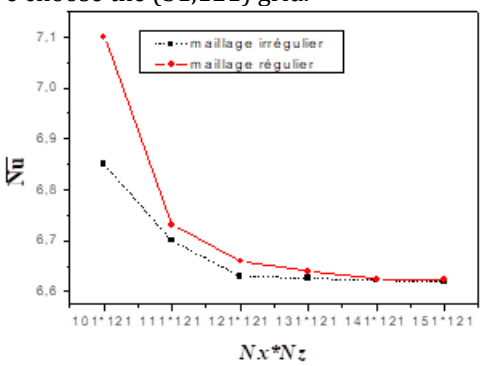

Figure 2: Influence of the grid on the heat transfer

The precision of our results are evaluated by adapting our numerical model to T.N.Anderson et al. [6] system; Fig. 3 show the variation of electrical (a) and thermal (b) efficiency with the ratio of the reduced temperature and global incident radiation on the collector surface.

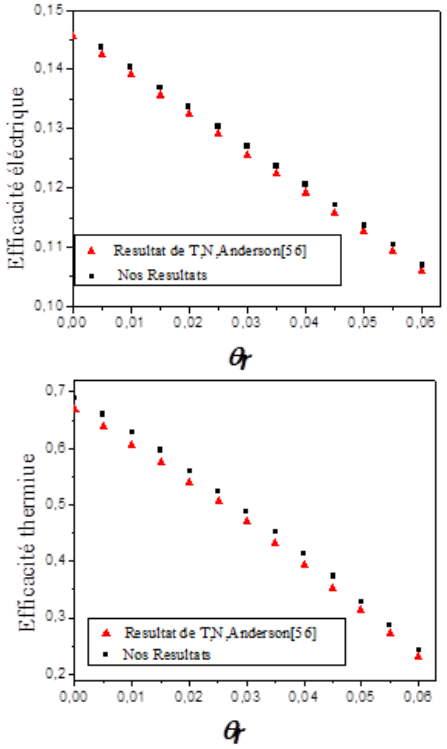

Figure 3: Comparison of our results with those of T.N.Anderson et al. [6] for absorber conductivity, λ = 135W/mK

Parametric analysis

➢ *Solar radiation effect*

The direct solar radiation captured by the PV sensor is characterized by the Rayleigh number $Ra_0 = \frac{g\beta I^*}{\lambda \vartheta a} H^4$, part of which will be transferred to the coolant and part of which will be transferred to the room.

We study the effect of the captured solar flux(Ra_0) on the average heat transfer (Nusselt number), to the vertical planes of the area occupied by heat transfer fluid (liquid gallium) at position X = 0.3 and the local at position X = 0. 7. Figure 4 shows the evolution of the average heat transfer ($\overline{Nu}$), in the vertical planes of the area occupied by the heat transfer fluid at position X = 0.3 and of the channel at position X = 0.7, and this in function of the solar flux captured by the front face of the PV sensor, Ra0. It can be seen that the heat transfer increases as a function of Ra_0 in both planes. Also we note that the difference between the two amounts of heat transferred increases with the solar flux collected.

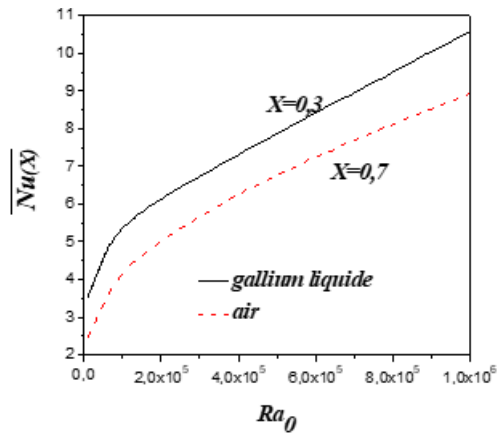

Figure 4: Influence of heat flux captured by the PV sensor on the heat transfer in the area occupied by the heat transfer fluid (X = 0.3) and the room (X = 0.7), for ***A*** = 1; E_m = 0.05 and L_{pm} = 0.1

Effect of injection speed

Figure. 5 illustrates the temperature profiles at the three remarkable positions: in the zone occupied by the gel (EVA: ***Pr*** = 0.05), on the rear face of the PV cells and in the zone occupied by the heat transfer fluid (gallium: ***Pr*** = 0.025) and at the channel (air: ***Pr*** = 0.71), for: Gr_{T0} = 1.41.10^6, L_{pm} = 0.1, E_m = 0.05, A = 1 and for different values of Reynolds number, Re. We note that near the photovoltaic cells (in the area occupied by the gel (EVA)) and also in the area occupied by the heat transfer fluid (gallium), when the speed of injection of air into the channel (Re) increases the value of the temperature decreases. In addition, this variation is the same in the zone of the channel nevertheless the temperature increases to 0.43 (corresponds to T = 32 ° C in the real case), while in the other zones does not exceed 0.25 (corresponds to T = 29 ° C in the real case). This is explained by the fact that when Re increases the residence time of the air in the channel decreases, but the heat flow transmitted by the coolant increases and accumulates and captures the maximum of heat lost by the Joule effect. Similarly, we see that the best value of the Reynolds number is the unit where the cell temperature is 0≤θ≤0.25 (0≤T≤29 ° C) and that at the channel 0≤θ≤0.43 (0≤T ≤32 ° C).

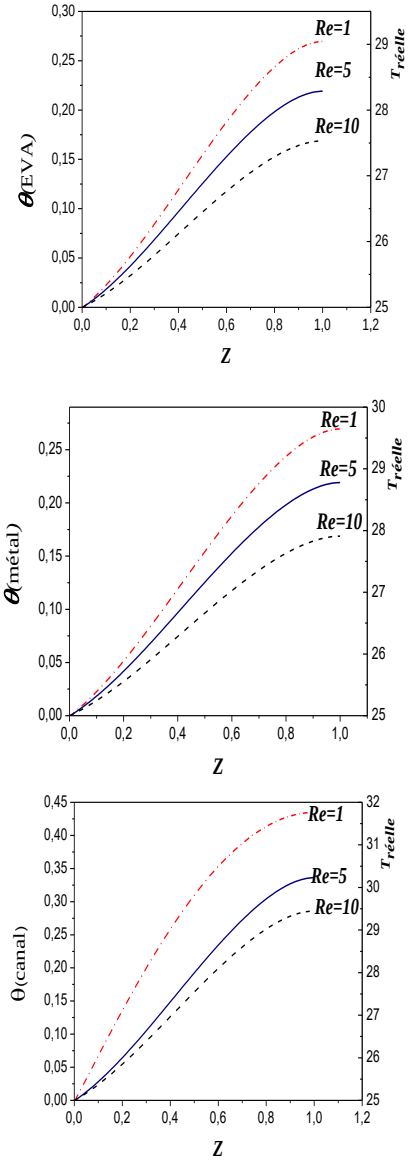

Figure 5 : Effect of the injection speed on the temperature profiles with: (a) in the zone occupied by the gel (EVA), (b) in the zone occupied by the heat transfer fluid, (c) at the channel for: Gr_{T0}=1.4110^6, *A=1*, L_{pm}=0.1, E_m=0.05.

Figure. 6 represents the evolution of the average heat transfer ($\overline{Nu}$) in the vertical plane of the channel at position X = 0.7 (air: ***Pr*** = 0.71), and this as a function of the speed of injection of air into the channel, ***Re***. It can be seen that the heat transfer decreases as a function of ***Re***, while keeping an important value compared to that transferred in the case of the closed room.

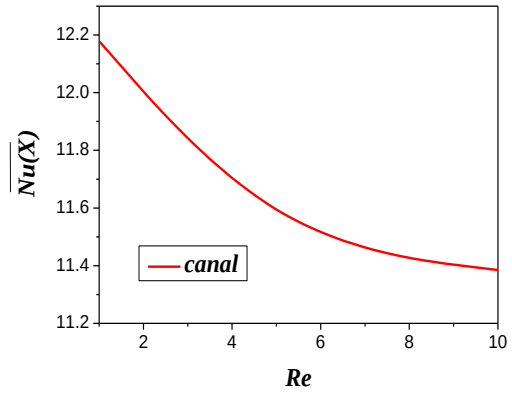

Figure 6: Influence of the speed of injection of air into the channel on the heat transfer, to the vertical plane of the channel (X = 0.7), for*: Gr_{T0}=1.4110⁶, A= 1 ; E_m=0.05 et L_{pm}=0.1.*

Effect of the thermal conductivity of the metal wall

After transmission of the heat from the heat transfer fluid to the wall which forms the partition between the PV sensor and the medium to be heated, this heat must be transmitted to the air passing through the channel. To do this, this partition must be metallic, because only metals have good heat conduction coefficients (copper: λ = 400; aluminum: λ = 237; steel: λ = 46).
For this purpose we have shown, for different types of metal wall (copper: pour = 400; aluminum: λ = 237; steel: λ = 46), the electrical and thermal efficiency of the PVT system as a function of the defined reduced temperature. As following :

$$\theta_r = \frac{\theta_{Tf_c} - \theta_{pf_c}}{I^*}$$

With: θ_{Tf_c} the temperature at the Tedlar / heat transfer fluid interface, θ_{pf_c} the temperature at the heat transfer fluid / metal wall interface and I^* the incident solar flux.

For this study, we have assumed that PV cells have a maximum efficiency of 18% (typical of a commercial crystalline silicon photovoltaic cell) at room temperature and as it varies with temperature, we propose to use the relation following given by [56].

- Electrical efficiency:

$$\eta_{el}(\theta_{cm}) = 0.18(1 - 0.005(\theta_{cm} - \theta_a))$$

With θ_{cm} : the average temperature of the N PV cells located in the j[th] column and θ_a a room temperature.

$$\theta_{cm} = \frac{1}{N}\sum_{i=1}^{N}\theta(j_c, i)$$

Similarly, the thermal efficiency as a function of the temperature of the metal absorber can be estimated by the following relation given by [56].

- Thermal efficiency:

$$\eta_{th(\theta_{am})} = F_R((\tau\alpha)_{PV}\beta_c + (1-\beta_c)(\tau\alpha)_a) - F_R U_{loss}\theta_{am}$$

With θ_{am}: the average temperature of the metal absorber located in the j[th] column.

$$\theta_{am} = \frac{1}{N}\sum_{i=1}^{N}\theta(j_a, i)$$

where F_R is the elimination efficiency.

Figure 7 (a), shows that the increase in the value of the thermal conductivity of the metal wall induces an increase in thermal efficiency, while respecting the rule that the latter decreases when the reduced temperature increases.

Figure 7 (b) shows that the increase in the value of the thermal conductivity of the metal wall induces a remarkable increase in electrical efficiency.
Indeed, the integration of the heat exchanger, menu of heat transfer fluids and metal wall with optimal thermal characteristics, improves the heat transfer to the channel.

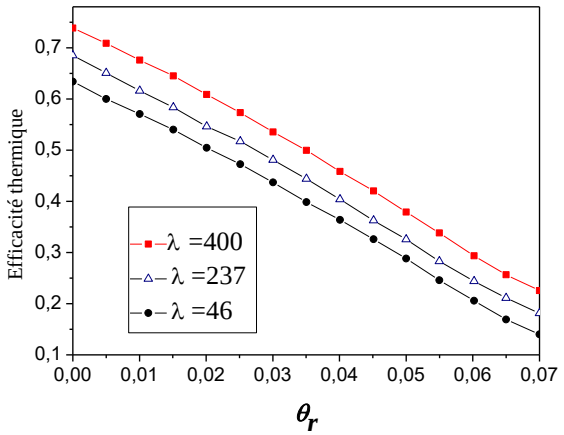

Figure 7 : The efficiency: (a) thermal and (b) electrical of the system relative to the reduced temperature for different values of the conductivity of the metal wall for : Gr_{T0}=1.4110⁶, L_{pm}= 0.1; A=1; E_m=0.05.

Conclusion

In this article, we have highlighted the effects of all the characteristic parameters of such a PVT system while trying to determine their optimal values which guarantee us a maximum heat exchange between the PV cells and the considered heat exchanger. Indeed, we have developed a model allowing to know beforehand, for each value of the applied heat flux, Ra_0, and that of the fluid injection speed, **Re**, the thermal and dynamic behavior of the different fluid and solid heat transfer fluids used. The profiles are analyzed as a function of the thickness of the metal wall, E_m, the width of the area between the PV panel and the metal plate, L_{pm}, the nature of the heat transfer fluid, **Bi**, and the thermal conductivity of the metal wall, **λ** . Such a validated model can be used as a tool for predicting results and optimizing the characteristic parameters of flow and transfer. We were able to select the appropriate heat

transfer fluids, namely liquid gallium and copper, allowing the cells to be cooled as much as possible and benefit from the heat lost by Joule effects to other utilities such as heating a room or a fluid crossing a canal.

References

[1] B. K. Koyunbaba, Z. Yilmaz, The comparison of trombe wall systems with single glass, double glass and PV panels, Renewable Energy. 45 (2012) 111-118.
[2] D. Kamthania, S. Nayak, G.N. Tiwari, Performance evaluation of a hybrid photovoltaic thermal double pass facade for space heating , Energy and Buildings. 43 (2011) 2274–2281.
[3] F.Sarhaddi, S. Farahat, A.Behzadmehr, Exergetic performance assessment pf a solar photovoltaic thermal (PV/T) air collector, Energy and Buildings. 42 (2010) 2184-2199.
[4] I.R. Caluianu, F. Baltaretu, Thermal modelling of a photovoltaic module under variable free convection conditions, Applied Thermal Engineering. 33-34 (2012)86-91.
[5] A. Ibrahim, M. Y. Othman, M. H. Ruslan, S.Mat, K. Sopian, Recent advances in flat plate photovoltaic/ thermal (PV/T) solar collectors, Renewable and Sustainable Energy Reviews. 15 (2011) 352-365.
[6] T.N. Anderson,M. Duke, G.L. Morrison, J.K. Carson, Performance of a building integrated photovoltaic/thermal (BIPVT) solar collector, Solar Energy. 83 (2009) 445-455.
[7] GL. Jin, A. Ibrahim, YK. Chean, R. Daghigh, H. Ruslan, S. Mat, et al., Evaluation of single-pass photovoltaic-thermal air collector with rectangle tunnel absorber, A.J.of Applied Sciences. 7 (2010) 277-282.
[8] B. Blocken, T. Defraeye, D. Derome, J. Carmeliet, High-resolution CFD simulations for forced convective heat transfer coefficients at the façade of a low-rise building, Buildingand Environment. 44 (2009) 2396-2412.
[9] T. Defraeye, B. Blocken, J. Carmeliet, CFD analysis of convective heat transfer at the surfaces of a cube immersed in a turbulent boundary layer, I. J. of Heat and Mass transfer . 53 (2010) 297-308.
[10] P. Karava, C. Mohammad Jubayer, E. Savory, Numerical modelling of forced convective heat transfer from the inclined windward roof of an isolated low-rise building with application to photovoltaic/thermal systems, Applied Thermal Engineering. 31 (2011) 1950-1963.
[11] R. Daghigh, A. Ibrahima, G. L. Jin, H. Ruslan, K. Sopian, Predicting the performance of amorphous and crystalline silicon based photovoltaic solar thermal collectors, Energy Conversion and Management. 52 (2011) 1741–1747.
[12] A. Ibrahima, MY. Othman, H. Ruslan, MA. Alghoul, Yahya, A. Zaharim, et al., Performance of photovoltaic thermal collector (PVT) with different absorbers design, WSEAS Trans Environ Develop. 5(3) (2009) 321–330.
[13] V. Roman, GN. Tiwari, Life cycle cost analysis of HPVT air collector under different Indian climatic conditions, Energy Policy. 36 (2008) 603-611.
[14] V. Roman, GN. Tiwari, A comparison study of energy and exergy performance of a hybrid photovoltaic double-pass and single-pass air collector, Int J Energy Res. 33 (2009) 605-617.
[15] S. Dubey, GS. Sandhu, GN. Tiwari, Analytical expression for electrical efficiency of PV/T hybrid air collector, Appl Energy. 86 (2009) 697-705.
[16] T. T Chow, G. Pei, KF. Fong,Z.Lin, ALS. Chan, J.Ji, Energy and exergy analysis of photovoltaic-thermal collector with and without glass cover, Applied Energy. 86(3) (2009) 310-6.
[17] S. Patankar, Numerical Heat Transfer and Fluid Flow, New York, 1980.
[18] J.P.Van Doormaal, G.D. Raithby, Enhancements of the simple Method for predicting incompressible fluid flows, Numerical Heat Transfer. 7 (1984) 147-163.
[19] D. Gobin, R. Bennacer, Cooperating thermosolutal convection in enclosures .2. Heat-transfer and flow structure, Heat and Mass Transfer, 39(13), (1996), 2683-2697